JOURNAL OF GEOPHYSICAL RESEARCH, VOL. 102, NO. B7, PAGES 15,151–15,161, JULY 10, 1997

The 1994-1995 seismicity and deformation at the Hengill triple junction, Iceland: Triggering of earthquakes by minor magma injection in a zone of horizontal shear stress

Freysteinn Sigmundsson,[1] Páll Einarsson,[2] Sigurdur Th. Rögnvaldsson,[3] G. R. Foulger,[4] K. M. Hodgkinson,[4] and Gunnar Thorbergsson[5]

Abstract. Since July 1994 an unusually persistent swarm of earthquakes ($M < 4.0$) has been in progress at the Hengill triple junction, SW Iceland. Activity is clustered around the center of the Hrómundartindur volcanic system. Geodetic measurements indicate a few centimeters uplift and expansion of the area, consistent with a pressure source at 6.5 ± 3 km depth beneath the center of the volcanic system. The system is within the stress field of the south Iceland transform zone, and the majority of the recorded earthquakes represent strike-slip faulting on subvertical planes. We show that the secondary effects of a pressure source, modeled as a point source in an elastic half-space, include horizontal shear that perturbs the regional stress. Near the surface, shear stress is enhanced in quadrants around the direction of maximum regional horizontal stress and diminished in quadrants around the direction of minimum regional stress. The recorded earthquakes show spatial correlation with areas of enhanced shear. The maximum amount of shear near the surface caused by the expanding pressure source exceeds 1 μstrain, sufficient to trigger earthquakes if the crust in the area was previously close to failure.

Introduction

The Hengill triple junction in SW Iceland is the junction of the Reykjanes Peninsula oblique rift, the western rift zone of Iceland, and the south Iceland transform (Figure 1). The three plates meeting at this junction are the North American plate, the Eurasian plate, and the Hreppar microplate located between the overlapping western and eastern rift zones in south Iceland. Left-lateral shear has been measured across the Reykjanes Peninsula [*Sturkell et al.*, 1994], as well as regional tilting towards the central axis of seismic activity on the Peninsula [*Tryggvason*, 1974]. Left-lateral shear is also accumulating across the south Iceland seismic zone where the majority of the ~2 cm/yr of relative plate motion appears to be accommodated [*Sigmundsson et al.*, 1995]. This shearing is driven by extension across the eastern rift zone in Iceland and shearing across the Reykjanes Peninsula. Currently, little extension is occurring across the western rift zone in Iceland [*Sigmundsson et al.*, 1995]. However, repeated leveling shows that this zone is currently subsiding at rates of one to several millimeters per year [*Tryggvason*, 1974; *Thorbergsson and Vigfússon*, 1990; *Czubik*, 1989].

The Hengill triple junction is named after the Hengill central volcano, which is the main volcanic production focus of the area, and is associated with a high-temperature geothermal area. The central volcano and its transecting fissure swarm, extending from the coast south of Hengill to north of Lake Thingvallavatn, form the Hengill volcanic system. Another active but less pronounced volcanic system, the Hrómundartindur volcanic system, lies at the eastern edge of the Hengill system, outside the Hengill fissure swarm (Figure 2a). The area near Mt. Hrómundartindur can be classified as the central volcano of this system; it is a separate focus of volcanic production with high geothermal activity [*Árnason et al.*, 1987; *Saemundsson*, 1992]. The geothermal activity and the concentration of CO_2 and H_2 in fumarole gases are most intense a few kilometers south of Mt. Hrómundartindur, at Ölkelduháls (Figure 2a) [*Árnason*, 1993; *Ívarsson*, 1996]. Seismic tomography of the uppermost 5 km of the crust has imaged the underlying heat source, a high-velocity body at 2-5 km depth beneath Ölkelduháls, interpreted as dense intrusives that represent a solidified shallow crustal magma chamber [*Foulger and Toomey*, 1989; *Foulger et al.*, 1995]. The most recent eruption in the Hrómundartindur volcanic system occurred about 10,000 years ago, whereas at least two major rifting events associated with extensive fissure eruptions have occurred in the Hengill system since then [*Saemundsson*, 1995].

Background seismicity occurs continuously throughout the Hengill triple junction and consists of continuous, small-magnitude earthquakes (Figure 2a) [*Foulger and Einarsson*, 1980; *Foulger*, 1988a], the majority of which have non-double-couple focal mechanisms interpreted as resulting from cooling contraction cracking due to circulating groundwater in hot rock at depth [*Foulger and Long*, 1984; *Foulger*, 1988b; *Miller*, 1996]. In July 1994 an unusually persistent

[1]Nordic Volcanological Institute, University of Iceland, Reykjavik.
[2]Science Institute, University of Iceland, Reykjavik.
[3]Icelandic Meteorological Office, Reykjavik.
[4]Department of Geological Sciences, University of Durham, Durham, England.
[5]National Energy Authority, Reykjavik.

Paper number 97JB00892.
0148-0227/97/97JB-00892$09.00

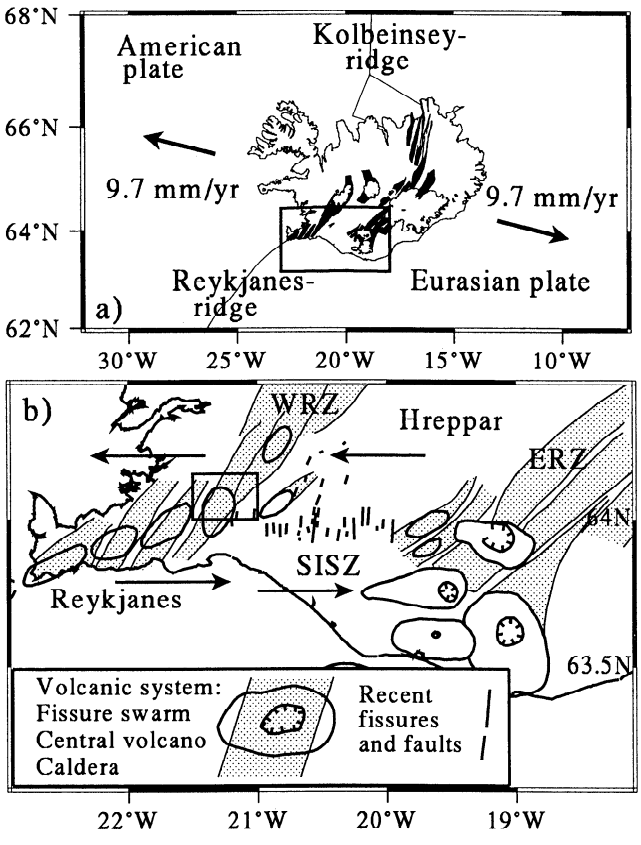

Figure 1. (a) Volcanic systems of Iceland (black areas); box denotes the location of Figure 1b. (b) Tectonic setting of the Hengill triple junction, the meeting point of the Reykjanes Peninsula oblique rift, the western rift zone (WRZ), and the south Iceland seismic zone (SISZ), which is a transform zone. Also shown is the eastern rift zone (ERZ) in Iceland and the Hreppar microplate between the western and eastern rift zones. Box denotes the study area shown in Figure 2. Arrows show schematically how the area north of the SISZ and the Reykjanes Peninsula moves currently to the west along with the North American plate and the area to the south moves to the east along with the Eurasian plate.

earthquake swarm began at the Hengill triple junction, with earthquakes clustered in the Hrómundartindur volcanic system (Figure 2b). Earthquake activity and seismic moment release remained at a highly elevated level in 1995 but declined in 1996. Geodetic measurements suggest a few centimeters of uplift and expansion of the area, consistent with a pressure increase at 6.5 ± 3 km depth beneath the center of the Hrómundartindur volcanic system. Spatial and temporal correlation of enhanced seismicity and inflation, at a center of a volcanic system, suggests that the common cause is magmatic movements. In particular, it has been demonstrated that inflation of a magma chamber can trigger earthquakes [e.g., *Thatcher and Savage*, 1982]. We show that flow of magma toward a still-molten bottom part of the otherwise frozen magma chamber identified in the Hrómundartindur volcanic system may have triggered at least some of the enhanced seismicity there. An alternative model, calling for dike injection at depth, is unlikely for several reasons. Dike injections in Iceland (e.g., at Krafla [*Einarsson and Brandsdottir*, 1980]) and other areas of basaltic volcanism are usually catastrophic; they are completed in hours and days, not months and years as the 1994-1995 earthquake swarm in the Hengill-Hrómundartindur area. Also, dike injections are associated with harmonic tremor and spatially migrating earthquake activity, signifying the propagation of a dike tip. The 1994-1995 earthquake swarm has none of these characteristics, suggesting dike injection did not occur.

Seismicity and Deformation

In the 18 month period from July 1, 1994, to December 31, 1995, about 12,000 earthquakes of moment magnitude $M_W \geq 0.5$ occurred in the Hengill-Hrómundartindur area between 64.0°-64.15°N and 21.0°-21.5°W (Figures 2b and 2c). The seismicity is described in detail by *Rögnvaldsson et al.* [1996]. The largest event was M_W 3.9, but 50 of the earthquakes have $M_W \geq 3.0$. The mean seismic rate in this period was 153 $M_W \geq 0.5$ earthquakes per week. For comparison, in the 18 month period of normal activity from January 1, 1993, to July 1, 1994, the mean seismic rate was 13 $M_W \geq 0.5$ earthquakes per week in the same area, and only 2 of the events exceeded M_W 3.0. Noticeable characteristics of the unusual seismic activity include its continuity since July 1994, the stability of the enhanced seismic moment release since February 1995 (Figure 3), and the small magnitudes of the earthquakes. Location uncertainty of the earthquakes is typically 1-1.5 km horizontally and 4 km vertically [*Rögnvaldsson et al.*, 1996]. Although our vertical location uncertainty is too great to infer the depth distribution of the 1994-1995 earthquakes, a study of previous earthquakes [*Foulger*, 1988a; *Foulger*, 1995] shows that earthquakes within the area originate from about 2 to 6 km depth.

Several lines of evidence suggest that the 1994-1995 earthquake swarm in the Hengill-Hrómundartindur area occurred in a zone of horizontal shear stress. Automatic focal mechanism evaluation [*Rögnvaldsson and Slunga*, 1993] of earthquakes in 1994 and 1995 are consistent with the majority of them being strike-slip events on subvertical planes, but normal faulting is also common (Figure 2c). Fault planes determined by relative location of similar earthquakes in the 1994-1995 swarm, as described by *Slunga et al.* [1995], are subvertical and strike mostly either N-S or E-W, in agreement with the strike-slip focal mechanisms. Also, regional Global Positioning System (GPS) geodetic measurements in south Iceland indicate that the study area is within a zone of horizontal shear strain [*Sigmundsson et al.*, 1995]. Furthermore, as described later in this paper, the spatial distribution of seismicity can be explained by a simple model if the study area is within a zone of horizontal shear stress. The direction of the maximum compressive stress axis, inferred from about 8500 earthquakes of $M_W \geq 0.5$, is N53°E, with a scatter of few degrees [*Rögnvaldsson et al.*, 1996]. It is within 10° of that observed in the south Iceland seismic zone [*Stefánsson et al.*, 1993].

Recent geodetic measurements detect small but significant uplift near the Hrómundartindur volcanic system. Repeated leveling in 1992-1995 detects up to 16 ± 3 mm of uplift along an 18 km long E-W directed profile from station A through B to C (Figures 2a and 4). In the period 1986-1994, up to 15 ± 2 mm uplift is observed along another 7 km long profile in N-S direction from station B to D (Figures 2a and 5).

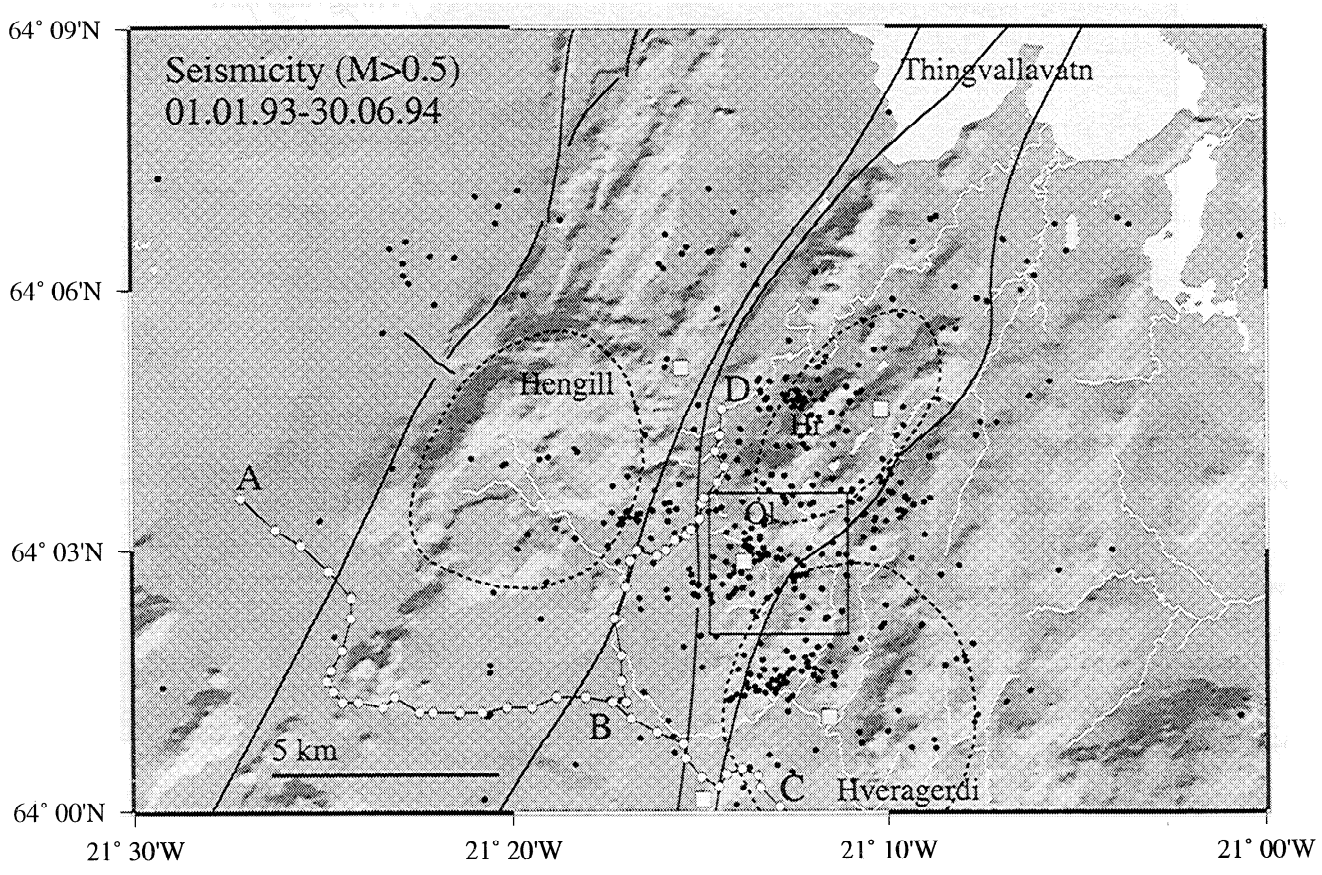

Figure 2a. $M_w > 0.5$ seismicity in the normal-activity period from January 1, 1993, to June 30, 1994 (black dots). Background map shows shaded topography of the Hengill area, illuminated from the SE. The 800 m high Mt. Hengill is the highest mountain in the area. Also marked are Mt. Hrómundartindur (Hr), Ölkelduháls (Ol), Lake Thingvallavatn and rivers in white, and the village of Hveragerdi. Limits of the Hengill and Hrómundartindur volcanic systems are shown with solid lines; dashed lines delineate the central volcanoes [after *Árnason et al.*, 1986]. Leveling profiles are shown by open dots connected by lines. The ABC profile (from station A through B to C) is approximately E-W oriented, and the BD profile (from station B to D) is approximately N-S oriented. A Mogi source located somewhere within the 3 × 3 km^2 area shown as a square box can explain observed elevation changes along the leveling profiles. The five small open squares denote GPS stations.

During each survey the leveling lines were measured both forward and backward using invar scale rods and lines of sight of about 30 m. The one standard deviation uncertainty of each survey is estimated to be 0.6 mm × $\sqrt{L}$, where L is the distance along the leveling line in kilometers [*Thorbergsson and Vigfússon,* 1990].

We test if the observed elevation changes can be explained as a response to a local pressure increase within the crust. According to *Anderson* [1936] and *Mogi* [1958] a point source of pressure in an elastic half-space (a Mogi model) leads to horizontal, u_r, and vertical, u_z, displacements, given by

$$u_r = C\frac{r}{(d^2+r^2)^{3/2}} \quad (1)$$

and

$$u_z = C\frac{d}{(d^2+r^2)^{3/2}} \quad (2)$$

where d is the source depth, r is the horizontal radial distance from the source, and C is the source strength parameter (Figure 6). The source strength parameter, C, is given by

$$C = \frac{3a^3\Delta P}{4\mu} = h_o d^2 \quad (3)$$

where ΔP is the change in fluid pressure within the sphere, a is the radius of the spherical source, μ is the rigidity of the crust surrounding the sphere, and $h_o = u_z(r=0)$. We locate a best fitting point source by conducting a systematic forward grid search, minimizing the difference between observed and predicted changes in the least squares sense. Elevations of benchmarks are not independent random variables, because they are the sum of elevation differences between benchmarks along a level line. To avoid this correlation of errors we follow *Vasco et al.* [1990] and model only the temporal changes in the elevation differences between successive benchmarks along the leveling lines. These are independent random variables. The average uncertainty in temporal change in elevation differences between adjacent benchmarks is estimated to be $\sigma_{average} = \sqrt{2} \times 0.6$ mm × $\sqrt{0.49}$ = 0.6 mm, where the average distance between permanent benchmarks is 0.49 km. For each of the repeated leveling lines we minimize the χ^2 function

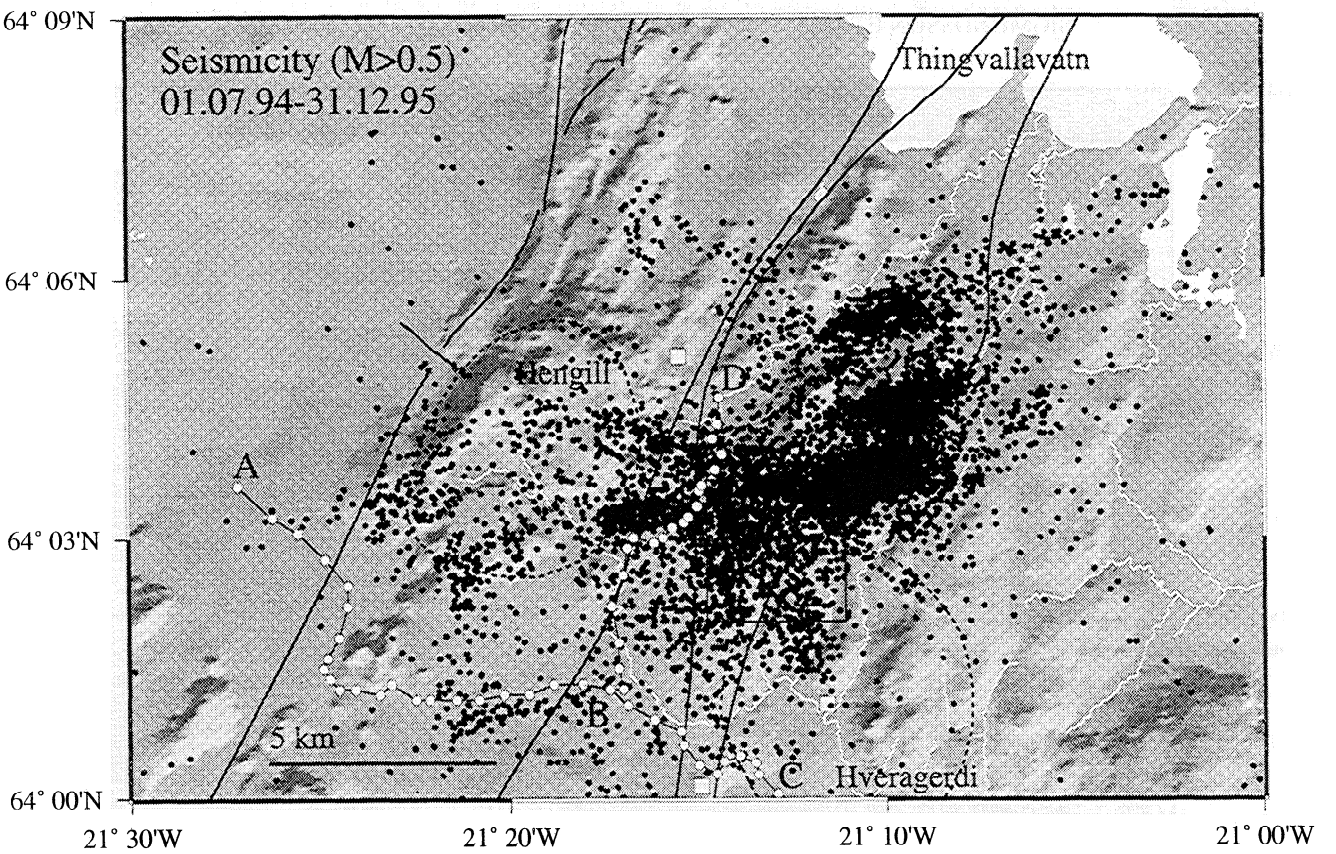

Figure 2b. $M_w > 0.5$ seismicity in the July 1, 1994, to December 31, 1995, period of greatly enhanced seismicity (black dots). Background map same as in Figure 2a. Several clusters are apparent within the swarm, aligned in ENE-WSW direction. These lineaments may represent weaknesses in the crust, but their direction is not reflected in the surface geology, and major faults with this direction are not known in the area.

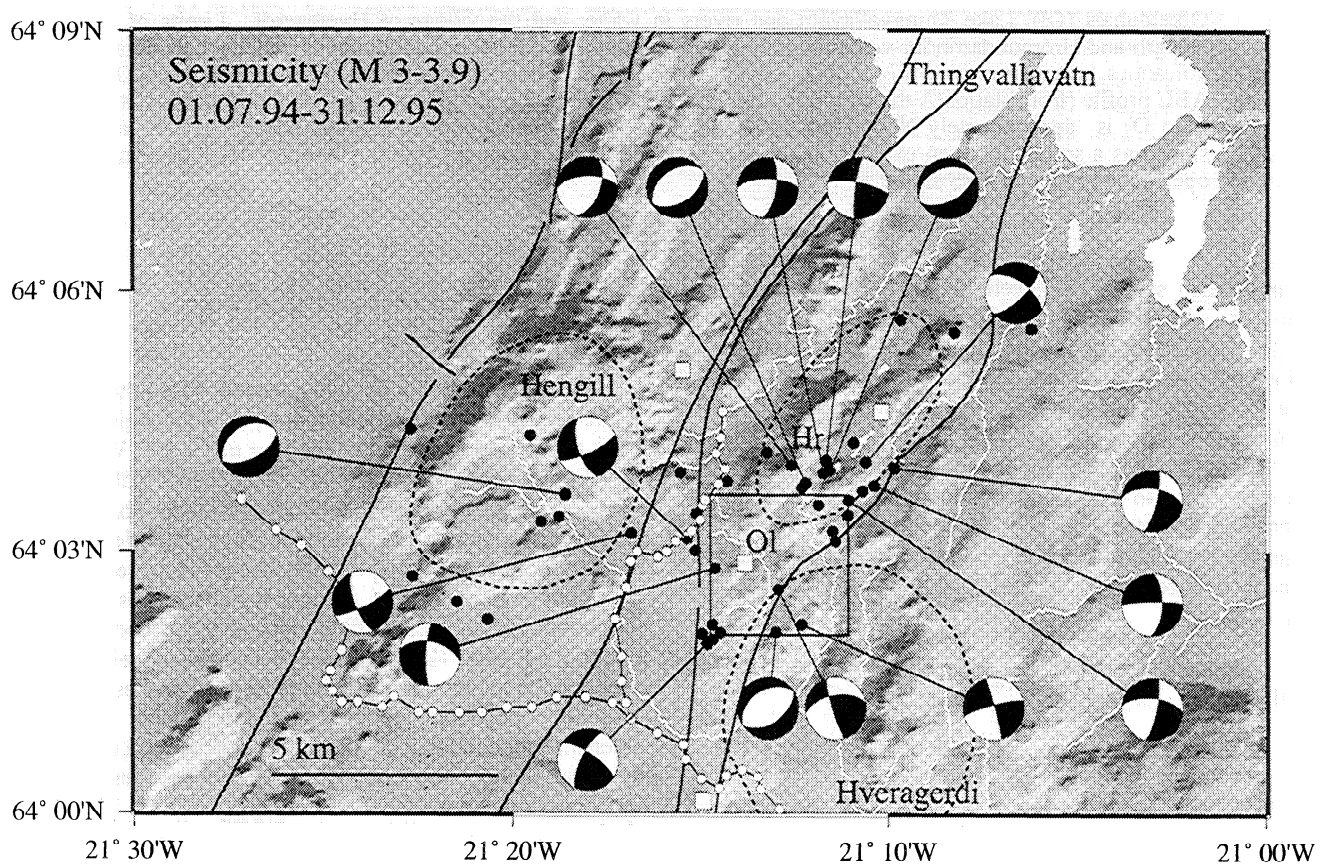

Figure 2c. Same as Figure 2b, except $M_w \geq 3.0$. The largest event is $M_w = 3.9$. Focal mechanisms of selected events are shown.

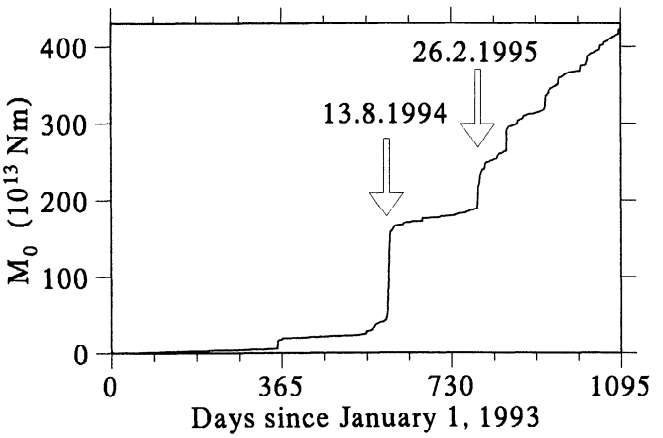

Figure 3. Seismic moment release versus time in the study area since January 1, 1993. The enhanced seismic activity began in July 1994, with the two largest swarms occurring in August 1994 and February 1995. The continuous, high-moment release after that is noticeable. The total moment released 1993-1995 is equivalent to a single $M_W = 5.6$ event.

$$\chi^2 = \sum_{i=2}^{N} \left(\frac{(\Delta h_i - \Delta h_{i-1})^{observed} - (\Delta h_i - \Delta h_{i-1})^{predicted}}{\sigma_{average}} \right)^2 \quad (4)$$

where Δh_i is the change in elevation of benchmark i between two surveys, observed or predicted by (2), and N is the number of benchmarks (36 for the ABC profile, 21 for the BD profile). We search for a single pressure source in a fixed location that can explain deformation along both profiles. We allow for different source strengths during the different observation periods of the profiles, 1986-1994 and 1992-1995. Assuming no model, then $\chi^2 = 504$. The best fit parameters of our point source model yield $\chi^2 = 280$, but we accept a model as a candidate explanation of the deformation if it yields a χ^2 value lower than 315. In that case, according to a statistical F test of significance [*Chatfield*, 1983] the observed and residual deformation are different at the 95% confidence level. On the basis of this criterion, a point source located at 64.0475°N ± 1.5 km, 21.2150°W ± 1.5 km and at a depth of 6.5 ± 3 km explains the observations. The source strength parameter for the 1992-1995 period is twice as large as the source strength for the 1986-1994 period. We assume that the pressure increase begins in the 1992-1994 period and continues in 1994-1995. On the basis of this, a best fit is obtained if central uplift, h_o, is equal in the two periods, $h_{o,1992\text{-}1994} = h_{o,1994\text{-}1995} = 2.5$ cm. The inferred 1992-1995 uplift is then 5 ± 2 cm (Figure 6). The integrated volume of model uplift is $2\pi h_o d^2 = 13 \times 10^6$ m^3. The relation between volume of uplift and volume of magma injection depends on Poisson's ratio of the crust and whether the incoming magma is emplaced directly in the crust or within a magma chamber, because of magma compressibility [e.g., *Sigmundsson et al.*, 1992]. In any case, the volume of injected magma is of similar order as volume of uplift, that is ~0.01 km^3. If the measurement errors have been correctly estimated and the single point source model is a complete model for the observed deformation, then the reduced χ^2 value, $\chi^2/(N-M)$, where N is the total number of observations and M is number of model parameters, should be ~1. In our case it is ~5, suggesting that either the measurement errors have been underestimated approximately by a factor of $\sqrt{5}$ (e.g., because of unstable benchmarks) or our model is incomplete. The largest model misfit is on the northern part of the BD leveling profile (Figure 5), where short-wavelength excessive uplift is observed. In that area the leveling profile crosses the 1994-1995 epicentral cluster (Figure 2b) and approaches the Ölkelduháls geothermal area. The misfit may be due to displacements on faults activated during the earthquake swarm, or due to near-surface changes in geothermal activity.

Further constraints on recent crustal deformation in the Hengill area are provided by GPS geodetic measurements. A network of 23 GPS stations covering the Hengill triple junction was initially measured in 1991 [*Hodgkinson and Foulger*, 1994]. We remeasured five of these stations in May 1995, and the data were analyzed in a similar manner as described by *Sigmundsson et al.* [1995]. In 1991 these stations were occupied for about 8 hours; the average 1σ

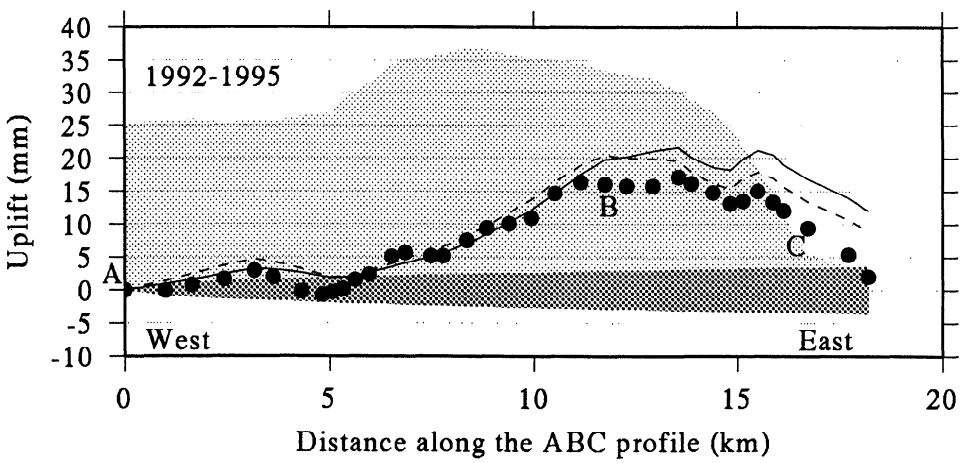

Figure 4. Uplift, relative to station A, from 1992 to 1995 versus distance along the ABC profile (dots) [*Thorbergsson and Vigfússon*, 1995]. Also shown is topography in tens of meters along the profile (light shading), and accumulated 1σ random error from station A (dark shading). Dashed line is model uplift (relative to station A) fitted to data from this profile only, solid line is model prediction using data from both the ABC and the BD leveling profiles. See Figure 2a for location of profiles.

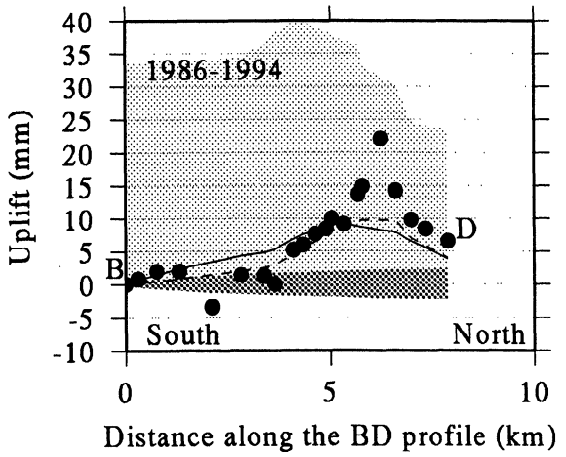

Figure 5. Uplift, relative to station B, from 1986 to 1994 versus distance along the BD profile (dots) [*Thorbergsson and Vigfússon*, 1994]. Otherwise same as Figure 4, except the time period and the reference station are different.

uncertainty of the horizontal components was less than 10 mm, and the average 1σ vertical uncertainty was less than 20 mm [*Hodgkinson and Foulger*, 1994]. Better satellite visibility and 20 hour long observation times in 1995 yielded still more accurate results with average horizontal and vertical

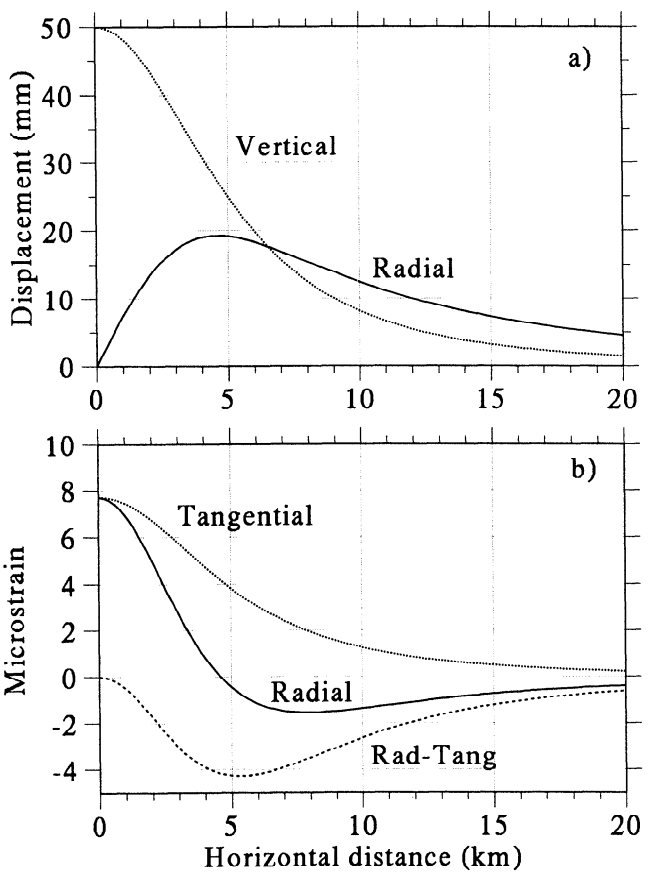

Figure 6. Surface displacements and strains 1992-1995 according to the best fit Mogi model. (a) Radial (u_r) and vertical (u_z) displacements. (b) Radial strain (ε_r), tangential strain (ε_t), and the difference between radial and tangential strain (ε_r-ε_t).

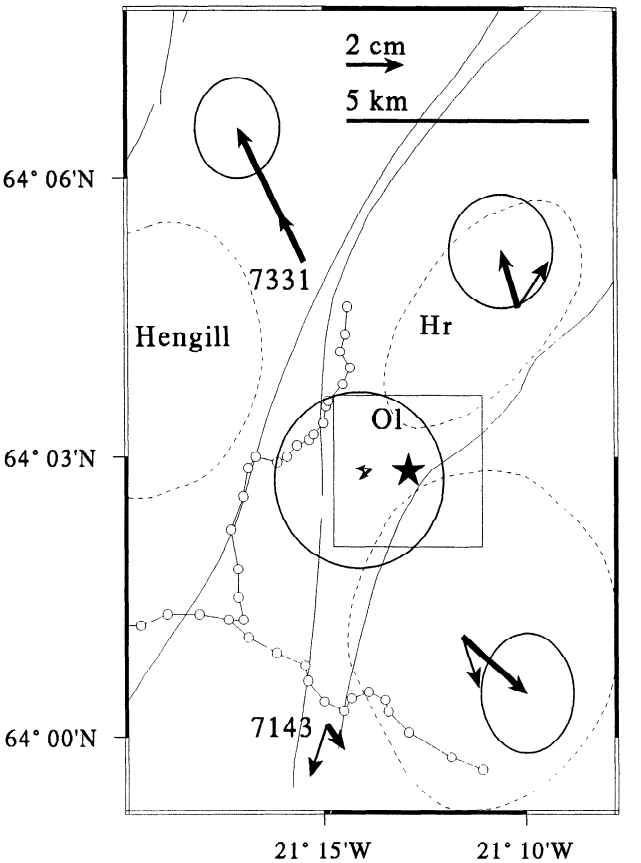

Figure 7. Observed horizontal displacements (thick arrows) of five GPS stations 1991-1995 with estimated 95% confidence limits, assuming a displacement of 10.6 mm in 144° direction at station 7143. Displacements were derived relative to the reference station 7143, then a constant vector was added to the displacements to minimize the sum of all the squared displacement vector lengths. Background map same as for Figure 2, except for the shading. Star shows the location of the Mogi source that best fits the leveling data and the square box is its admissible location range. Thin arrows are horizontal model displacements due to this source. Residual displacements partly reflect regional left-lateral shear accumulation across the area. The large misfit at station 7331 may suggest deviation from the spherical magma chamber source geometry assumed in the Mogi model, or it may be a local effect (e.g., related to nearby geothermal activity).

uncertainties of 4 and 8 mm. Inferred horizontal displacements 1991-1995 (Figure 7) indicate areal expansion of a few centimeters, consistent with the leveling results. The direct inclusion of these observations into the inversion for the best fit pressure source is complicated by the fact that the pressure changes at depth are not the sole contributor to horizontal deformation. Left-lateral shearing in an east-west direction across the study area is also to be expected, as in the nearby south Iceland seismic zone. Vertical displacements estimated from GPS range from -6 to 23 mm but do not correlate with elevation changes predicted by the model. However, the predicted vertical deformation is within the 95% confidence limits of the GPS estimates of vertical elevation change. Furthermore, the GPS measurements exclude models that predict significantly greater elevation changes than those inferred from the leveling.

Enhancement of Shear Stress by a Point Source of Pressure

Our seismic and geodetic measurements show spatial and temporal correlation of gradual inflation and enhanced earthquake activity, and we suggest that inflation of a magma chamber may have triggered the earthquakes. Pressure change in a magma chamber will cause a change of stress in the surrounding crust. Consider a spherical magma chamber of radius a in an unbounded elastic material and increase the pressure in it by ΔP. The maximum compressive principal stress is $\sigma_1 = \Delta P(r_* / a)^{-3}$ in a radial direction from the center of the source, where r_* is the radial distance from the source. The other two principal stress components are $\sigma_2 = \sigma_3 = -0.5\Delta P(r_* / a)^{-3}$ in planes perpendicular to σ_1 [*McTigue*, 1987]. Increased pressure in a spherical chamber therefore leads to a local stress field such that in the chamber roof the maximum stress is vertical and compressive and horizontal stresses are extensional. Normal faulting is favored. For magma chambers at shallow depths in the crust the effects of the free surface of the Earth have to be considered. The compressive vertical stress goes to zero at the free surface but horizontal stresses continue to be extensional above the chamber. Normal faulting is favored there, as well as for deep chambers. Because of the cylindrical symmetry, the fault planes have no preferred strike direction. A well-documented example of normal faulting seismicity above an expanding pressure source is at the Phlegraean Fields caldera at Pozzuoli Bay Italy. From mid-1982 until September 1984 the caldera rose ~1.6 m at an average rate of about 2 mm/day [*Berrino et al.*, 1984]. At the same time, seismicity in the central area of the uplift was dominated by normal faulting on planes with no predominant strike direction [*Gaudiosi and Iannaccone*, 1984]. In the Hengill-Hrómundartindur area we observe a somewhat different relation between enhanced seismicity and inflation. Important aspects of the enhanced seismicity there that require explanation are that the majority of the earthquakes are strike-slip events on N-S and E-W fault planes and that the earthquakes are unevenly distributed around the inflation source (Figure 2b). Earthquakes mostly occur NE and SW of the inflation source; much fewer earthquakes occur NW and SE from the source. This is due to the location of the inflation source within a regional zone of horizontal shear, as we demonstrate by analyzing shear strain caused by a Mogi source and consider how it adds to regional shear.

The secondary effects of a Mogi pressure source include horizontal shear. Horizontal radial strain, ε_r, and horizontal tangential strain, ε_t, are given by

$$\varepsilon_r = \frac{\partial u_r}{\partial r} = C\frac{d^2 - 2r^2}{(d^2 + r^2)^{5/2}} \tag{5}$$

$$\varepsilon_t = \frac{1}{r}\frac{\partial u_t}{\partial \varphi} + \frac{u_r}{r} = C\frac{1}{(d^2 + r^2)^{3/2}} \tag{6}$$

where φ is azimuth and other parameters have been previously defined. During inflation, ε_t is positive at all distances, but ε_r crosses zero at $r = d/\sqrt{2}$ (Figure 6). If these near-surface principal strains are rotated into an x-y coordinate system [*Turcotte and Schubert*, 1982, p. 95], the surface strain tensor becomes

$$\mathbf{T}_{mogi} = \begin{bmatrix} \varepsilon_{xx} & \varepsilon_{xy} \\ \varepsilon_{yx} & \varepsilon_{yy} \end{bmatrix}$$

$$= \begin{bmatrix} \varepsilon_r \cos^2\varphi + \varepsilon_t \sin^2\varphi & 0.5(\varepsilon_r - \varepsilon_t)\sin 2\varphi \\ 0.5(\varepsilon_r - \varepsilon_t)\sin 2\varphi & \varepsilon_r \sin^2\varphi + \varepsilon_t \cos^2\varphi \end{bmatrix} \tag{7}$$

where

$$\varepsilon_r - \varepsilon_t = C\frac{-3r^2}{(d^2 + r^2)^{5/2}} \tag{8}$$

The x-y coordinate system is here defined such that the origin is at the Mogi source, the x axis points east, the y axis points north, and φ is the anticlockwise angle from the x axis. The ε_{xy} shear strain will depend on both distance and direction from the source.

The value of the shear strain is lower than the value of ε_{xx} and ε_{yy} (equation (7) and Figure 6), and horizontal shearing is therefore a secondary effect. However, its effect can become important if the pressure source is located within a regional zone of horizontal shear stress. If this shear zone is close to failure, small shear stresses added by a pressure source can easily trigger earthquakes. Assume an east-west oriented zone of width L where left-lateral simple shear strain accumulates because the block north of it moves to the west and the block south of it moves to the east. In the same x-y coordinate system as for the pressure source, the regional strain state is

$$\mathbf{T}_{regional} = \begin{bmatrix} 0 & -0.5u/L \\ -0.5u/L & 0 \end{bmatrix} \tag{9}$$

where u is the cumulative relative displacement across the shear zone since the last major earthquake sequence that released stresses. In (9), left-lateral shear is negative. In terms of principal strains this regional strain field is alternatively described by $\varepsilon_1 = 0.5u/L$ in direction N45°E and $\varepsilon_2 = -0.5u/L$ in direction N45°W. Consider now a pressure source located within this shear zone. If the regional strain field is stronger than the local strain field caused by a pressure source, then the local field acts as a perturbation on the regional field. The directions of the strain axis in the combined field are approximately the same as in the regional field, and the total combined shear strain is approximately

$$\varepsilon_{xy} = \varepsilon_{yx} = \varepsilon_{xy,regional} + \varepsilon_{xy,Mogi} = \frac{-u}{2L} + \frac{\varepsilon_r - \varepsilon_t}{2}\sin 2\varphi$$

$$= \frac{-u}{2L} + \frac{-h_o}{2d}\frac{3(r/d)^2}{(1 + (r/d)^2)^{5/2}}\sin 2\varphi \tag{10}$$

In our example the regional left-lateral shear strain is enhanced NE and SW of the pressure source, in quadrants around the direction of maximum regional horizontal stress, and diminished NW and SE of the pressure source in quadrants around the direction of minimum regional stress (Figure 8). The above example applies directly to the Hengill-Hrómundartindur area, as it is within an east-west oriented zone of left-lateral shear. The strain enhancement caused by the Mogi source will increase stress on subvertical strike-slip faults, depending on their orientation. In our case the stress increase will be maximum on faults oriented N-S

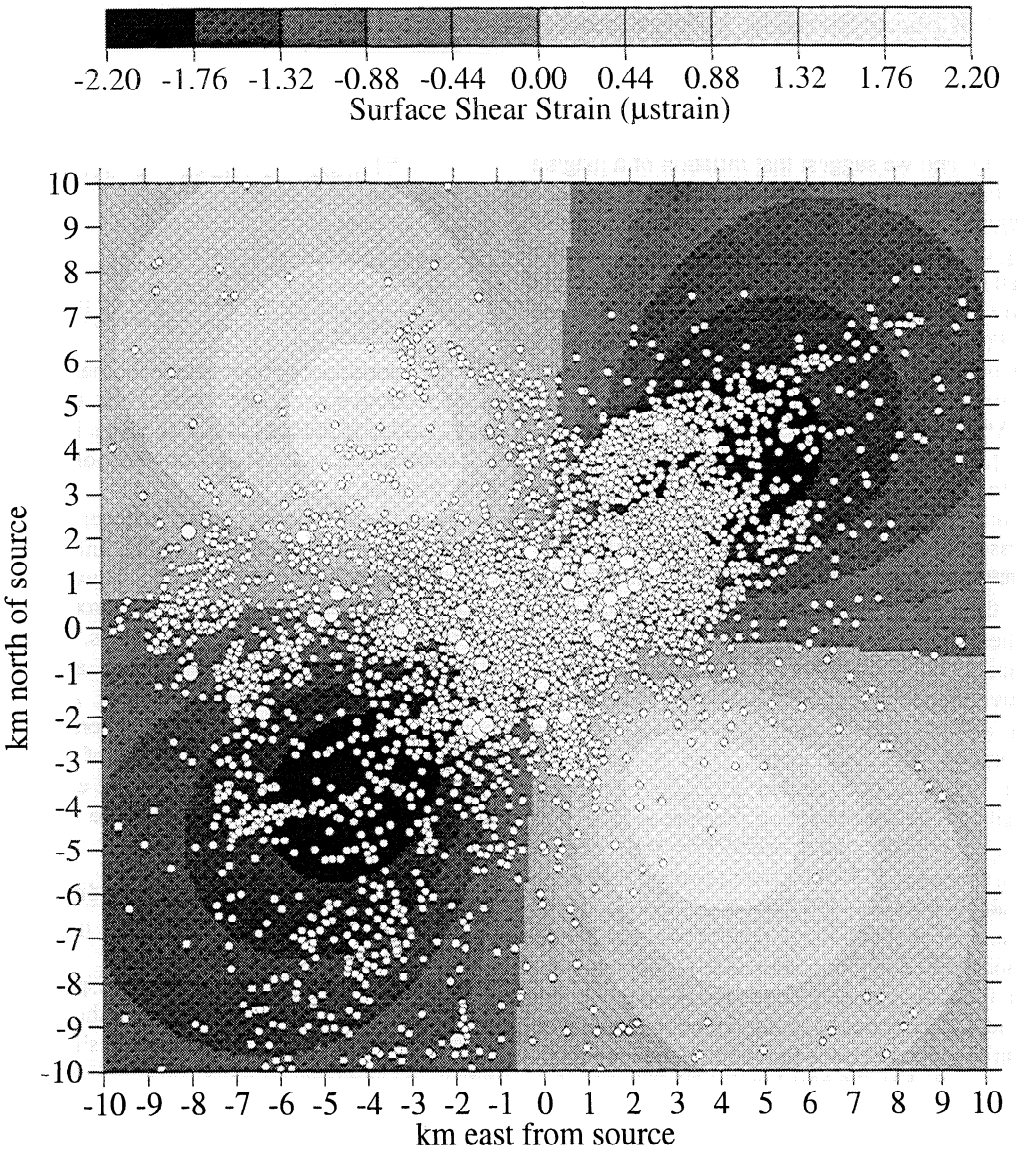

Figure 8. Surface shear strain added by a Mogi point source of pressure to regional shear strain according to (10). Source depth of 6.5 km and a central uplift of 5 cm is assumed. Left-lateral shear in an E-W direction, as the regional shear strain, is negative. Areas with high negative values are the areas of amplified regional shear strain. The axis of maximum amplification is the same as the axis of maximum regional compression which is orientated N53°E in the study area. Epicenters of $0.5 \leq M_w < 3.0$ earthquakes from July 1, 1994, to December 31, 1995, are plotted as small white dots and $M_w \geq 3.0$ as large white dots. The pressure source is here assumed to be located 750 m north of the best fit location on the basis of geodetic data but well within the geodetically inferred admissible range of the source location.

and E-W. Within the 1994-1995 earthquake swarm, this was the dominant type of failure.

Discussion

The persistency of the 1994-1995 enhanced activity at the Hengill triple junction is very unusual. Such a long episode of enhanced small-magnitude earthquake activity is seldom observed in Iceland, and in particular, no activity of similar length has been recorded before on the Reykjanes Pensinsula, the south Iceland seismic zone, nor the western volcanic zone. The current activity resembles in many ways increased earthquake activity at volcanoes in response to increase of magma pressure at depth. An example is enhanced earthquake activity of the Krafla volcano in north Iceland in the years 1974 and 1975, activity that preceded the 1975-1984 Krafla rifting episode when multiple eruptions and dike injections occurred. From autumn 1974 to December 20, 1975, earthquake activity at the Krafla volcano remained at an exceptionally high level, the largest earthquakes approached M 4, and they were rather evenly distributed in time [*Einarsson*, 1991; *Björnsson et al.*, 1977]. The prerifting seismic activity is thought to have been a consequence of accumulation of magma at shallow depth within the Krafla volcano which caused increased magma-chamber pressure, leading to tens of centimeters surface doming of the Krafla volcano [*Möller and Ritter*, 1980; *Ritter*, 1982]. Observed deformation within our study area is

an order of magnitude smaller than at Krafla, and we do not believe that the current level of activity signals an impending rifting event.

The long duration and stability of the 1994-1995 earthquake activity suggests that it was sustained by something more than plate-motion strain accumulation. Increased pressure beneath the Hrómundartindur volcanic system, possibly related to magma injection there, is a candidate trigger that is consistent with the observations. The geodetic data are consistent with a pressure increase at depth near the center of the Hrómundartindur volcanic system. Such a pressure increase is most easily explained by accumulation of magma at shallow depths, a process that is known to be important at central volcanoes in general. A high-velocity body imaged at 2-5 km depth beneath Ölkelduháls was interpreted by *Foulger and Toomey* [1989] and *Foulger et al.* [1995] as a frozen magma chamber. Our inferred pressure source lies below this high-velocity body and could be a still-molten part of a mostly solidified magma chamber that has received a modest inflow of magma from depth. Our geodetic data suggests ~0.01 km^3 of magma has been injected into the Hrómundartindur system. This corresponds to a spherical volume with a radius of ~130 m. This is a small volume when compared to the volume of magma involved in rifting events and eruptions in Iceland (e.g., at the Krafla and Hekla volcanoes during this century).

The study area is within the stress field of the south Iceland seismic zone, in a zone of horizontal shear. Earthquakes occur because the northern part of the study area is moving to the west, relative to the southern part of the study area, causing left-lateral shear. We have shown that a pressure source will enhance such shearing in quadrants, radiating from the pressure source, in the direction of the maximum compressional stress. As the areas of increased shear show spatial correlation with recorded earthquakes (Figure 8), our hypothesis provides an explanation for the distribution and spatial extent of the earthquake activity. We do not expect a perfect correlation between our simple model calculation and the distribution of earthquakes for the following two reasons: (1) we only estimate change in shear stress near the surface, whereas the pattern is a function of depth and (2) we have not considered the effect of confining pressure on friction on faults [*King et al.*, 1994; *Stein et al.*, 1994]. By considering these effects, it is likely that the distribution of earthquakes may be explained in some more detail than we have done.

Our explanation requires high stress in the study area before the pressure increase; the crust must have been close to failure. The level of stress there can be expected to be related to the regional level of stress within the nearby south Iceland seismic zone. That zone is currently near the end of an earthquake cycle, a sequence of M 6 - M 7 earthquakes is anticipated there within the next 20 years, whereas no $M = 7$ earthquakes have occurred there since 1912 [*Einarsson et al.*, 1981]. A high level of regional stress within both the south Iceland seismic zone and the Hengill-Hrómundartindur area is thus expected. The predicted surface shear caused by the point source is significant when compared to the likely rate of regional shearing in the study area. The rate of left-lateral shearing across the south Iceland seismic zone is about 2 cm/yr across about 25 km wide zone, or about 0.8 μstrain/yr on average [*Sigmundsson et al.*, 1995]. The Hengill area is north of the zone of maximum shearing, so regional shearing there may be somewhat lower. The maximum surface shearing inferred from the point source model is more than 2 μstrain and corresponds therefore to at least several years of plate-motion strain accumulation. For shear modulus of 3×10^{10} Pa, 2 μstrain correspond to shear stress of about 1.2 bars. Studies elsewhere in the world indicate this level of stress is more than sufficient to trigger earthquake activity [e.g., *Stein et al.*, 1994].

The recent activity in the Hrómundartindur volcanic system is comparable in many ways with 1989-1991 activity of the Long Valley Caldera in California documented by *Langbein et al.* [1993]. An episode of inflation began there in October 1989, when extensional strain rates increased from near 0 to 9 ppm/yr. Through the end of 1991, inflation amounted to about 11 cm. Seismic activity during this period was very similar to the recent activity in the Hrómundartindur volcanic system. Seismic activity increased by more than an order of magnitude, many events exceeded $M = 3.0$, and the largest event was $M \approx 4.0$. The geodetic network in the Long Valley Caldera, measured several times weekly using a two-color Geodimeter, shows that the onset of inflation preceded the onset of enhanced seismicity by about 2 months. Earthquakes were triggered by the inflation. Another example of similar activity as in the Hrómundartindur volcanic system may be at the Alban Hills Volcano, Italy [*Amato and Chiarabba*, 1995]. Frequent earthquake swarms and uplift at Alban Hills appear to be related to magma injection, despite no eruptive activity in the area during the last ~20,000 years.

Conclusions

A pressure source within a zone of horizontal shear can locally amplify shear stress and thereby trigger earthquake activity. Shear stress is enhanced in quadrants around the direction of maximum regional horizontal shear stress. The size of the affected area depends on source depth and strength, and the time history of the pressure increase controls the time history of seismicity. This model explains several features of the exceptional seismic activity observed in the period 1994-1995 at the Hengill triple junction, SW Iceland. A 6.5 ± 3 km deep source of gradually increasing pressure beneath the center of the Hrómundartindur volcanic system is consistent with (1) the spatial extent and distribution of seismicity, (2) the time history of the seismicity, and (3) the deformation observed by leveling and GPS measurements. The pressure source lies below gabbroic intrusives inferred from seismic tomography and may represent a still-molten part of a mostly solidified magma chamber that has received ~0.01 km^3 of magma from depth. The mechanism we propose cannot operate unless the stress level in the Hengill-Hrómundartindur area was close to failure prior to the magma injection. This is consistent with high stress in the nearby south Iceland seismic zone that is also believed to be close to failure.

Acknowledgments. This work was supported by Icelandic Research Council grants 95-N-080 and 957010096 and European Commission grant ENV4-CT96-0252. Comments from reviewers, Timothy H. Dixon and Pierre Briole, and an associate editor, Roger Bilham, helped us to significantly improve the paper. All figures were made with the public domain GMT software.

References

Amato, A., and C. Chiarabba, Recent uplift of the Alban Hills Volcano (Italy): Evidence for magmatic inflation?, *Geophys. Res. Lett., 22*, 1985-1988, 1995.

Anderson, M. E., Dynamics and formation of cone-sheets, ring-dykes, and cauldron-subsidence, *Proc. R. Soc. Edinburgh, 56*, 128-157, 1936.

Árnason, K., Jarðhiti á Ölkelduhálssvæði, viðnámsmælingar 1991 og 1992 (Geothermal Activity in the Ölkelduháls Area), in Icelandic with an English summary, *Rep. OS-97018/JHD-02*, Nat. Energy Auth., Reykjavik, Iceland, 1993.

Árnason, K., G. I. Haraldsson, G. V. Johnsen, G. Thorbergsson, G. P. Hersir, K. Saemundsson, L. S. Georgsson, and S. P. Snorrason, Nesjavellir, Jarðfræði- og jarðeðlisfræðileg könnun (Nesjavellir, Geological and geophysical investigations 1985), in Icelandic with an English summary, *Rep. OS-86014/JHD-02*, Nat. Energy Auth., Reykjavik, Iceland, 1986.

Árnason, K., G. I. Haraldsson, G. V. Johnsen, G. Thorbergsson, G. P. Hersir, K. Saemundsson, L. S. Georgsson, S. Th. Rognvaldsson, and S. P. Snorrason, Nesjavellir - Ölkelduháls, yfirborðskönnun (Surface Geology at Nesjavellir - Ölkelduháls), in Icelandic with an English summary, *Rep. OS-87018/JHD-02*, Nat. Energy Auth., Reykjavik, Iceland, 1987.

Berrino, G., G. Corrado, G. Luango, and B. Toro, Ground deformation and gravity changes accompanying the 1982 Pozzuoli uplift, *Bull. Volcanol., 47*, 187-200, 1984.

Björnsson, A., K. Saemundsson, P. Einarsson, and K. Grönvold, Current rifting episode in north Iceland, *Nature, 266*, 318-323, 1977.

Chatfield, C., *Statistics for Technology: A Course in Applied Statistics*, 3rd ed., 381 pp., Chapman and Hall, New York, 1983.

Czubik, E., Beobachtungen rezenter erdkrustenbewegungen: 650 km Feinnivellements in Island, *Z. Vermess., 114*, 25-33, 1989.

Einarsson, P., The Krafla rifting episode 1975-1989, in *Náttúra Mývatns* (The Nature of Lake Mývatn, in Icelandic), edited by A. Gardarson and Á. Einarsson, pp. 97-139, Icelandic Nature Sci. Soc., Reykjavik, 1991.

Einarsson, P., and B. Brandsdottir, Seismological evidence for lateral magma intrusion during the July 1978 deflation of the Krafla volcano in NE-Iceland, *J. Geophys., 47*, 160-165, 1980.

Einarsson, P., S. Björnsson, G. Foulger, R. Stefansson, and Th. Skaftadottir, Seismicity pattern in the south Iceland seismic zone, in *Earthquake Prediction: An International Review, Maurice Ewing Ser.*, vol. 4, edited by D. W. Simpson and P. G. Richards, pp. 141-151, AGU, Washington, D. C., 1981.

Foulger, G. R., Hengill triple junction, SW Iceland, 1, Tectonic structure and the spatial and temporal distribution of local earthquakes, *J. Geophys. Res., 93*, 13493-13506, 1988a.

Foulger, G. R., Hengill triple junction, SW Iceland, 2, Anomalous earthquake focal mechanisms and implications for process within the geothermal reservoir and at accretionary plate boundaries, *J. Geophys. Res., 93*, 13507-13523, 1988b.

Foulger, G. R., The Hengill geothermal area, Iceland: Variation of temperature gradients deduced from the maximum depth of seismogenesis, *J. Volcanol. Geotherm. Res., 65*, 119-133, 1995.

Foulger, G. R., and P. Einarsson, Recent earthquakes in the Hengill-Hellisheidi area in SW-Iceland, *J. Geophys., 47*, 171-175, 1980.

Foulger, G. R., and R. E. Long, Anomalous focal mechanisms: Tensile crack formation on an acceting plate boundary, *Nature*, 310, 43-45, 1984.

Foulger, G. R., and D. R. Toomey, Structure and evolution of the Hengill-Grensdalur volcanic complex, Iceland: Geology, geophysics, and seismic tomography, *J. Geophys. Res., 94*, 17511-17522, 1989.

Foulger, G. R., A. D. Miller, B. R. Julian, and J. R. Evans, Three-dimensional v_p and v_p/v_s structure of the Hengill triple junction and geothermal area, Iceland, and the repeatability of tomographic inversion, *Geophys. Res. Lett.*, 22, 1309-1312, 1995.

Gaudiosi, G., and G. Iannaccone, A preliminary study of stress pattern at Phlegraean Fields as inferred from focal mechanisms, *Bull. Volcanol., 47*, 225-231, 1984.

Hodgkinson, K. M., and G. R. Foulger, First epoch GPS survey of the Hengill triple junction, SW Iceland, and the effect of ocean loading, *Jökull, 44*, 17-27, 1994.

Ivarsson, G., Fumarole gas at Hengill: Sampling and analysis 1993-1995 (in Icelandic), internal report, Reykjavik Munic. Heat. Co., Reykjavik, 1996.

King, G. C. P., R. S. Stein, and J. Lin, Static stress change and the triggering of earthquakes, *Bull. Seismol. Soc. Am., 84*, 935-953, 1994.

Langbein, J., D. P. Hill, T. N. Parker, and S. K. Wilkinson, An episode of reinflation of the Long Valley Caldera, Eastern California: 1989-1991, *J. Geophys. Res., 98*, 15851-15870, 1993.

McTigue, D. F., Elastic stress and deformation near a finite spherical magma body: Resolution of the point source paradox, *J. Geophys. Res., 92*, 12931-12940, 1987.

Miller, A. D., Seismic structure and earthquake focal mechanisms of the Hengill volcanic complex, SW Iceland, Ph.D. thesis, Univ. of Durham, Durham, England, 1996.

Mogi, K., Relations between the eruptions of various volcanoes and the deformation of the ground surfaces around them, *Bull. Earthquake Res. Inst. Univ. Tokyo, 36*, 99-134, 1958.

Möller, D., and B. Ritter, Geodetic measurements and horizontal crustal movements in the rift zone of NE-Iceland, *J. Geophys., 47*, 110-119, 1980.

Ritter, B., Untersuchungen geodätischer Netze in Island zur Analyse von Deformationen von 1965 bis 1977, *Reiche C*, no. 271, Deutsche Geod. Komm., München, Germany, 1982.

Rögnvaldsson, S. Th., and R. Slunga, Routine fault plane solutions for local networks: A test with synthetic data, *Bull. Seismol. Soc. Am., 83*, 1232-1247, 1993.

Rögnvaldsson, S. Th., G. Gudmundsson, K. Ágústsson, R. Stefánsson, and S. Jakobsdóttir, Recent seismicity near the Hengill triple-junction, SW Iceland, in *Seismology in Europe*, Proceedings of the XXV General Assembly of the Eur. Seismol. Comm., edited by B. Thorkelson, pp. 461-466, Icelandic Meteorological Office, Reykjavik, Iceland, 1996.

Saemundsson, K., Geology of the Thingvallavatn area, *Oikos, 64*, 40-68, 1992.

Saemundsson, K., Hengill, geologic map (bedrock) 1:50,000, Nat. Energy Auth., Reykjavik, Iceland, 1995.

Sigmundsson, F., P. Einarsson, and R. Bilham, Magma chamber deflation recorded by the Global Positioning System: The Hekla 1991 eruption, *Geophys. Res. Lett., 19*, 1483-1486, 1992.

Sigmundsson, F., P. Einarsson, R. Bilham, and E. Sturkell, Rift-transform kinematics in south Iceland: Deformation from Global Positioning System measurements, 1986-1992, *J. Geophys. Res., 100*, 6235-6248, 1995.

Slunga, R., S. Th. Rögnvaldsson, and R. Böðvarsson, Absolute and relative location of similar events with application to microearthqaukes in southern Iceland, *Geophys. J. Int., 123*, 409-419, 1995.

Stefánsson, R., R. Bödvarsson, R. Slunga, P. Einarsson, S. Jakobsdóttir, H. Bungum, S. Gregersen, J. Havskov, J. Hjelme, and H. Korhonen, Earthquake prediction research in the south Iceland seismic zone and the SIL project, *Bull. Seismol. Soc. Am., 83*, 696-716, 1993.

Stein, R., G. C. P. King, and J. Lin, Stress triggering of the 1994 M = 6.7 Northridge, California, earthquake by its predecessors, *Science, 265*, 1432-1435, 1994.

Sturkell, E., F. Sigmundsson, P. Einarsson, and R. Bilham, Strain accumulation 1986-1992 across the Reykjanes Peninsula plate boundary, Iceland, determined from GPS measurements, *Geophys. Res. Lett., 21*, 125-128, 1994.

Thatcher, W., and J. C. Savage, Triggering of large earthquakes by magma-chamber inflation, Izu Peninsula, Japan, *Geology, 10*, 637-640, 1982.

Thorbergsson, G., and G. H. Vigfússon, Landmaelingar á Nesjavöllum og Hengilsvæði 1982-1990 (Geodetic measurements at Nesjavellir and Hengill 1982-1990), in Icelandic, *Rep. OS-90046/VOD-07B*, Nat. Energy Auth., Reykjavik, Iceland, 1990.

Thorbergsson, G., and G. H. Vigfússon, Landmaelingar á Nesjavöllum og Hengilsvæði 1992 og 1994 (Geodetic measurements at Nesjavellir and Hengill 1992 and 1994), in Icelandic, *Rep. OS-94036/VOD-05B*, Nat. Energy Auth., Reykjavik, Iceland, 1994.

Thorbergsson, G., and G. H. Vigfússon, Fallmaeling á Hellisheidi og í Kömbum 1995 (Leveling at Hellisheidi and Kambar 1995),

in Icelandic, *Rep. OS-95049/VOD-07B*, Nat. Energy Auth., Reykjavik, Iceland, 1995.

Tryggvason, E., Vertical crustal movement in Iceland, in *Geodynamics of Iceland and the North Atlantic Area*, edited by L. Kristjánsson, pp. 241-262, D. Reidel, Norwell, Mass., 1974.

Turcotte, D. L., and G. Schubert, *Geodynamics*, John Wiley, New York, 1982

Vasco, D. W., R. B. Smith, and C. L. Taylor, Inversion for sources of crustal deformation and gravity change at the Yellowstone caldera, *J. Geophys. Res.*, *95*, 19839-19856, 1990.

P. Einarsson, Science Institute, University of Iceland, Dunhaga 5, IS-107 Reykjavik, Iceland. (e-mail: palli@raunvis.hi.is)

G. R. Foulger and K. M. Hodgkinson, Department of Geological Sciences, University of Durham, South Rd., Durham, DH1 3LE England, UK. (e-mail: g.r.foulger@durham.ac.uk)

S. Rognvaldsson, Icelandic Meteorological Office, Bustadavegur 9, IS-150 Reykjavik, Iceland. (e-mail: sr@vedur.is)

F. Sigmundsson, Nordic Volcanological Institute, University of Iceland, Grensasvegur 50, IS-108 Reykjavik, Iceland. (e-mail: fs@norvol.hi.is).

G. Thorbergsson, National Energy Authority, Grensasvegur 9, IS-108 Reykjavik, Iceland.

(Received July 9, 1996; revised February 25, 1997; accepted March 19, 1997.)